

Middle Cretaceous $p\text{CO}_2$ Variation in Yumen, Gansu Province and its Response to the Climate Events

LEI Xiangtong^{1, 2}, DU Zhen¹, DU Baoxia^{1, 2, *}, ZHANG Mingzhen³ and SUN Bainian¹

¹ School of Earth Sciences & Key Laboratory of Mineral Resources in Western China (Gansu Province), Lanzhou University, Lanzhou, 730000, China

² State Key Laboratory of Palaeobiology and Stratigraphy, Nanjing Institute of Geology and Palaeontology, Chinese Academy of Sciences, Nanjing 210008, China

³ Key Laboratory of Petroleum Resources, Gansu Province/Key Laboratory of Petroleum Resources Research, Institute of Geology and Geophysics, Chinese Academy of Sciences, Lanzhou 730000, China

Abstract: The palaeo-atmospheric CO_2 concentration ($p\text{CO}_2$) variation in the Yumen, Gansu Province during the middle Cretaceous has been reconstructed using the newly established plant photosynthetic gas exchange mechanistic model, and the results show that the $p\text{CO}_2$ values are in the range of about 550–808 ppmv. The present $p\text{CO}_2$ values are higher than the $p\text{CO}_2$ results (531–641 ppmv) of the previous study according to the Recent standardization of the stomatal ratio method, and much lower than the $p\text{CO}_2$ results (882–1060 ppmv) according to the Carboniferous standardization of the stomatal ratio method. The present $p\text{CO}_2$ variation is not only within the error range of GEOCARB II and GEOCARB III but also is similar to the reconstructed results based on the biochemistry and carbon isotope models. Besides, the present *Brachyphyllum* specimens were collected from four consecutive horizons of the upper Zhonggou Formation of the Hanxia Section, and the reconstructed $p\text{CO}_2$ exhibits the reconstructed $p\text{CO}_2$ exhibits a decline trend during the late Aptian to early Albian. This decline variation is probably associated with the Oceanic Anoxic Events (OAE1b) and the Cold snap event. With the combination of $p\text{CO}_2$ during the Albian to Cenomanian recovered by the plant photosynthetic gas exchange mechanistic model, the $p\text{CO}_2$ showed a prominent increase during the late Aptian to early Cenomanian, which indicates a response to the greenhouse warming during the middle Cretaceous. Therefore, the mechanical model of the plant photosynthetic gas exchange shows a relatively strong accuracy in the reconstruction of the $p\text{CO}_2$ and can reflect a strong relation between the atmospheric CO_2 concentrations and climatic events.

Key words: $p\text{CO}_2$, greenhouse climate, plant photosynthetic gas exchange mechanical model, OAE1b, Cold snap

1 Introduction

Middle Cretaceous is considered as a time of greenhouse climatic conditions during earth's history and also a vital time of transition of the global tectonics, environment, and climate, including profound influences to the earth's surficial environment from Massive oceanic volcanic activity (Larson, 1991; Jones, 2001), oceanic anoxic events (Schlanger and Jenkyns, 1976; Jenkyns, 1980), and magnetic quiet zone (Helsley and Maureen, 1968; Cronin et al., 2001). The greenhouse gas carbon

dioxide (CO_2) is not only one of the fundamental driving forces that regulate climate but also is the second largest significant greenhouse gas after water vapor (Grein et al., 2013); it plays an important role in adjusting surface temperatures in geological history (Came et al., 2007; Huang et al., 2012). Thus, credible CO_2 concentration data will help to clarify the palaeoclimate and palaeoenvironment. The atmospheric CO_2 concentration has been increasing rapidly since modern times due to the human activities (Mehrotra et al., 2003). Researches indicate that the global atmospheric CO_2 concentration has increased by 30% with global warming (Royer et al., 2004; Mann et al., 1999, 2013). Hence, the reconstruction

* Corresponding author. E-mail: dubx@lzu.edu.cn

of atmospheric CO₂ concentration is crucially important for a better understanding of global climatic and environmental changes (Xie Shucheng et al., 2018).

The reconstruction of the palaeo-atmospheric CO₂ concentration (*p*CO₂) has received great attention and has been studied by many scholars. Since 1991, Berner et al. proposed and improved the geochemical models (GEOCARB I, GEOCARB II, GEOCARB III, and GEOCARB SULF). Based on these models, the atmospheric CO₂ concentration over the Phanerozoic period (Wang et al., 2014) was reconstructed. These models also provide a correction for estimating the *p*CO₂ levels in the Phanerozoic (Haworth et al., 2005; Aucour et al., 2008; Ren et al., 2008; Passalia, 2009; Du et al., 2016; Sun B.N et al., 2016; Sun Y.W et al., 2016; Dai and Sun, 2017). In addition, the isotopic compositions of boron in marine foraminifera (Katz et al., 2010), the isotopic compositions of carbon in pedogenic carbonate (Weislogel et al., 2008; Huang et al., 2012), and marine alkenones (Pagani, 2002), as well as the traditional stomatal methods based on the plant fossil stomatal index (SI) and stomatal ratio (SR), were used to reconstruct the *p*CO₂.

Of the numerous *p*CO₂ reconstruction methods, the traditional stomatal methods (SI and SR method) have been widely used to reestablish the concentration of atmospheric CO₂ in the past. These methods are based on the negative correlation between the stomatal parameters (stomatal density and SI) of fossil leaf cuticles and variation of atmospheric CO₂ concentrations (Kürschner et al., 1998; Bonis and Kürschner, 2010). While reconstructing *p*CO₂ using plant fossil, SI and SR are semiquantitative with many restrictions (Beerling et al., 2002, 2009; Konrad et al., 2008; Franks et al., 2009; Jordan, 2011; Grein et al., 2011, 2013; Roth-Nebelsick et al., 2014).

The SI method was summarized using a transfer function between the SI values of modern plants and variation in the atmospheric CO₂ levels, which was combined with herbarium specimens and ice-core records. Then, the transfer function was used to estimate the *p*CO₂ using the SI values of certain fossil plants (Retallack, 2001; Beerling, et al., 2002). The SI method requires a close relation between the fossil specimens and modern plants (Kürschner et al., 2008); otherwise, the SI would be extremely insensitive to the variation of the CO₂ concentration (Beerling et al., 2002). Moreover, the assumption that there have been no evolutionary shifts in ecology and physiology of these species over time must hold good. Thus, the SI method is largely limited to the *p*CO₂ reconstructions during the Cenozoic.

The SR method is a feasible indicator for the reconstruction of atmospheric CO₂ concentration

throughout the geological time (Wang et al., 2014); the reconstructed *p*CO₂ results are presented as minimum and maximum values and are reconstructed by two different standards (recent and Carboniferous standardization). The SR method is mainly based on the SR values, which are calculated based on stomatal index of the nearest living equivalent species to the fossil plants (McElwain and Chaloner, 1995; Wang et al., 2014). The SR method is widely used to estimate the *p*CO₂ levels during the Mesozoic (Aucour et al., 2008; Du et al., 2016; Haworth et al., 2005; Passalia, 2009; Ren et al., 2008; Sun Y.W et al., 2016; Dai and Sun, 2017).

Recently, the mechanistic models based on the leaf gas exchange during photosynthesis have been widely applied to reconstruct the *p*CO₂ of the past. Konrad et al. (2008) proposed the mechanistic theoretical model based on the stomatal data, photosynthesis, and gas exchange control (Sun B.N et al., 2016). Many scholars have used this model to estimate the *p*CO₂ levels in the Cenozoic (Grein et al., 2011, 2013; Roth-Nebelsick et al., 2012, 2014; Sun B.N et al., 2016). The precondition to using this method is that the temperature during the plant growth period should be above 10°C, because the optimum temperature of woody plants for photosynthesis ranges between 10°C–35°C (Grein et al., 2013; Roth-Nebelsick et al., 2014; Sun B.N et al., 2016). It is obvious that palaeoclimatic parameters (temperature and humidity) are important for the reconstruction of atmospheric CO₂ concentration using this model. As it is quite difficult to get an accurate temperature and humidity data of the Mesozoic, the model of Konrad et al. (2008) is limited in its scope.

Franks et al. (2014) established a new mechanistic model approach to predict the *p*CO₂ based on the stomata anatomic data and the carbon isotope data of the fossil leaves. A large number of experimental studies have found a relation between the atmospheric CO₂ and internal CO₂ within the leaves. This model takes full advantage of the substantive parameter, such as the stomata pore length and width, stomatal density that can represent the ability of leaf gas exchange, and the critical variables such as the carbon isotope data of fossil plants. Franks et al. (2014) reestablished the *p*CO₂ from Devonian to Miocene (395–10 Ma). This model has little restrictions and uncertainties on the palaeoclimatic parameters and therefore can be widely used to reconstruct the *p*CO₂ during the Mesozoic and Paleozoic.

Using the plant photosynthetic gas exchange mechanical model of Franks et al. (2014), the variation in atmospheric CO₂ concentrations during the early–middle Cretaceous (late Aptian–early Albian) of Yumen, NW Gansu Province were reconstructed again using the SR approach (Du et al., 2016). The estimated results were

then compared with previously published $p\text{CO}_2$ results to recover the $p\text{CO}_2$ variation during the middle Cretaceous. Furthermore, the relation between the related $p\text{CO}_2$ fluctuations and geological events during the middle Cretaceous are discussed.

2 Geological Settings

The Cretaceous strata in China are well developed, which provide many significant sites for Cretaceous plant fossils in the world (Deng Shenghui et al., 2012b; Li et al., 2016), and perfect materials for studying the change of the ecological environment (Jin et al., 2017). All examined specimens in this paper were collected from the upper unit of the Zhonggou Formation in the Hanxia Section, which is 30 km west of Laojunmiao County, Gansu Province, NW China (Fig. 1). The Zhonggou Formation consists of the calcareous-clastic sedimentary rock with a grayish green color (Zhang et al., 2015). According to the lithological and palaeobiological characteristics, the upper unit of Zhonggou Formation was divided into six members (Sun et al., 2013; Du et al., 2014; Du et al., 2016). The present fossil specimens were found in five depositional members (member 2–6). According to the single zircon U–Pb dating, the age of the Zhonggou Formation is about 115.0 ± 4.5 Ma (Li et al., 2013). When combined with the assemblages of macro-fossils and spore-pollen (Deng et al., 2005; Deng Shenghui and Lu Yuanzheng, 2008; Du et al., 2014, 2016; Zheng et al., 2015; Zhang et al., 2015), the age of the Zhonggou Formation is probably late Aptian to early Albian.

3 Samples and Methods

3.1 Plant material

The present fossil plants were assigned to the *Brachyphyllum* variant based on morphological and micro-morphological structures, which were studied carefully (Du et al., 2014). Some of the *Brachyphyllum* specimens were well preserved with cuticles. The cuticular fragments were treated using the traditional method (Du et al., 2014; Du et al., 2016), and the anatomic data of stomata (the pore length p , width l , and stomatal density D) were observed with a scanning electron microscope and measured using Photoshop CS6. All stomatal anatomy data from the *Brachyphyllum* in this paper are summarized in Table 1. Since the quantum of stomatal anatomic data does not meet the statistical requirements, the fossil plants' data from the members were abandoned. All specimens numbered are stored in the Paleontological Laboratory of the School of Earth Sciences, Lanzhou University, Lanzhou, China.

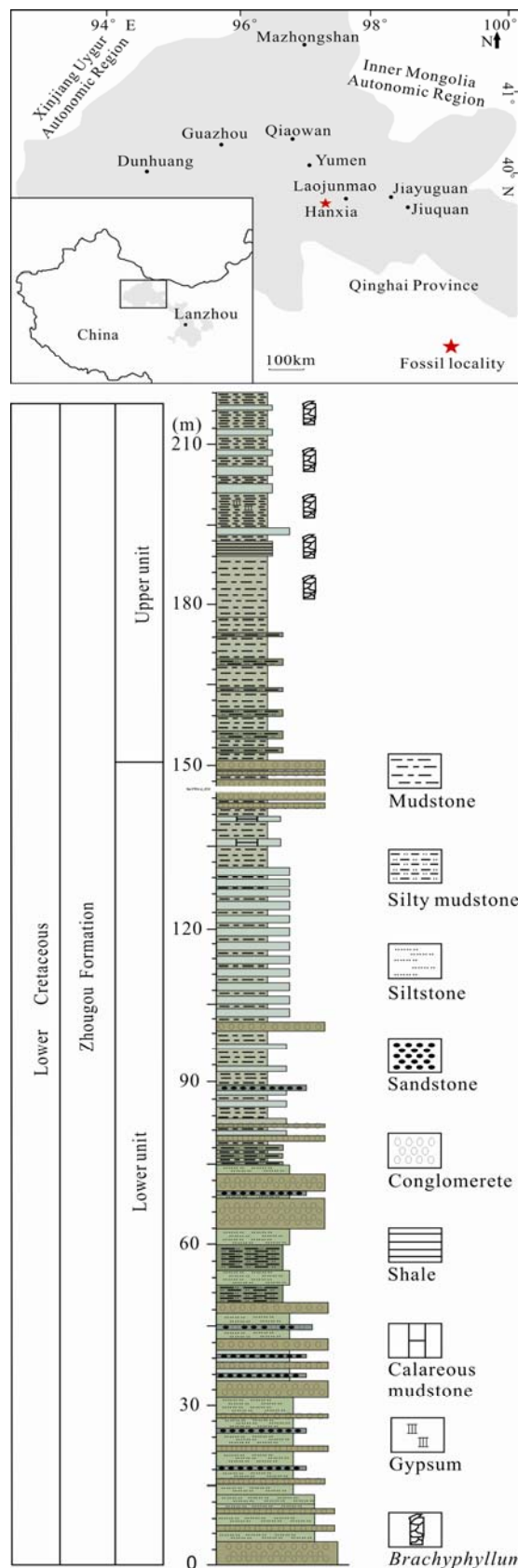


Fig. 1. The fossil site and stratigraphic column of the mid-Cretaceous Zhonggou Formation in Hanxia Section, Yumen, Gansu Province (modified from Du et al., 2014; Zhang et al., 2015).

3.2 Mechanistic model

The variation of atmospheric CO₂ concentration is a crucial factor in limiting enzyme reactions during photosynthesis, which directly changes in photosynthetic capacity and carboxylation efficiency by affecting the production of Rubisco (C₃ plants) and PEP carboxylase (C₄ plants) (Franks et al., 2012). Therefore, the atmospheric CO₂ concentration directly affects the rate of CO₂ assimilation by leaves (A_n , $\mu\text{mol m}^{-2} \text{s}^{-1}$) as an environmental variable. After a large number of experimental studies, a fundamental biophysical model of leaf gas exchange was established based on the response of gas exchange to atmospheric CO₂ concentration in the process of plant photosynthesis. This model assumed that the conditions and forms of photosynthetic gas exchange in past forests were similar to the modern forests. Hence, the ancient atmospheric CO₂ concentration (C_a , ppmv) can be calculated using the equations (1)–(8) that follow; this model was described and discussed in detail by Franks et al. (2014); thus, only a brief introduction is provided here.

$$C_a = \frac{A_n}{g_{c(\text{tot})} \cdot (1 - C_i/C_a)} \quad (1)$$

where $g_{c(\text{tot})}$ is the total stomatal conductance to CO₂, C_i is the internal CO₂ concentration in the leaf, and A_n is the CO₂ assimilation rate, which is described based on the relative change with respect to the long-term changes in C_a (Franks et al., 2013; Franks et al., 2014):

$$A_n \approx A_0 \left[\frac{(C_a - \Gamma^*)(C_{a0} + 2\Gamma^*)}{(C_a + 2\Gamma^*)(C_{a0} - \Gamma^*)} \right], \quad (2)$$

Where A_0 and C_{a0} are the reference values for A_n and C_a under the prevailing environmental conditions (A_0 , $10 \mu\text{mol m}^{-2} \text{s}^{-1}$; C_{a0} , 360 ppmv), and Γ^* is the CO₂ compensation point in the absence of dark (40 ppmv, 25°C).

$$g_{c(\text{tot})} = \left(\frac{1}{g_{cb}} + \frac{1}{g_{c(\text{op})}} + \frac{1}{g_m} \right)^{-1}. \quad (3)$$

This equation is equated and solved for $g_{c(\text{tot})}$, where g_{cb} is the conductance of leaf boundary layer to CO₂ ($2 \text{ mol}^{-1} \text{ s}^{-1}$); g_m is the conductance of mesophyll, $g_m = 0.013 \cdot A_n$ (Epron et al., 1995; Evans et al., 1996); $g_{c(\text{op})}$ is the conductance of operational stomatal ($g_{c(\text{op})} = \xi \cdot g_{c(\text{max})}$); the

mean ξ is 0.2 in field conditions for trees growing naturally).

$$g_{c(\text{max})} = \frac{d}{v} \cdot D \cdot a_{\text{max}} / \left(l + \frac{\pi}{2} \sqrt{a_{\text{max}}/\pi} \right) \quad (4)$$

$g_{c(\text{max})}$ is controlled by the stomatal size and stomatal density (D), which can also be expressed by equation (4) (Franks and Beerling, 2009). In addition, d and v are CO₂ diffusivity in air and the molar volume of air respectively; the parameter l presents the stomatal depth, while D is the stomatal density.

$$a_{\text{max}} = \beta \cdot (\pi p^2/4), \quad (5)$$

where a_{max} is the maximum stomatal aperture, which determines the length of the stomatal pore (p).

Therefore, C_i/C_a is solved from the relative carbon isotope composition of fossil leaves ($\delta^{13}C_{\text{leaf}}$) by the equations (6) and (7):

$$C_i/C_a = \left[\frac{\Delta_{\text{leaf}} - a}{b - a} \right], \quad (6)$$

$$\Delta_{\text{leaf}} = \frac{\delta^{13}C_{\text{air}} - \delta^{13}C_{\text{leaf}}}{1 + \delta^{13}C_{\text{leaf}}/1000}, \quad (7)$$

where a is the carbon isotope fractionation due to diffusion of CO₂ in air (4.4‰) (Farquhar et al., 1982), and b is the fractionation associated with RuBP carboxylase (taken as 30‰ here) (Roeske and O'Leary, 1984).

$$\delta^{13}C_{\text{air}} = (\delta^{13}C_{\text{leaf}} + 18.67)/1.10 \quad (8)$$

The isotopic composition of the atmospheric $\delta^{13}C_{\text{air}}$ was established by equation (8) (Arens et al., 2000).

4 Results

The $p\text{CO}_2$ of Yumen, Gansu Province is reconstructed again based on the fossil *Brachyphyllum* collected from four consecutive sedimentaries from the late Aptian to early Albian using the plant photosynthetic gas exchange mechanistic model approach of Franks et al. (2014); the estimated values were 550–808 ppmv. The related stomatal anatomic and carbon isotope data are summarized in Table 1. The estimated $p\text{CO}_2$ values based on the mechanistic model of Franks et al. (2014) is within the previous $p\text{CO}_2$ values recovered based on SR method (Du et al., 2016) and is higher than the $p\text{CO}_2$ reconstructed

Table 1 Stomatal anatomy data of *Brachyphyllum* and the estimated $p\text{CO}_2$ values from Yumen, Gansu Province

Member	Specimen number	P (μm)	D (mm^2)	L (μm)	β	a_{max} (m^2)	$g_{c(\text{max})}$ mol/ ($\text{m}^2 \cdot \text{s}$)	$g_{c(\text{op})}$ mol/ ($\text{m}^2 \cdot \text{s}$)	g_m mol/ ($\text{m}^2 \cdot \text{s}$)	g_{cb} mol/ ($\text{m}^2 \cdot \text{s}$)	$^{13}C_{\text{leaf}}$ (‰)	$^{13}C_a$ (‰)	C_i/C_a	A_0 $\mu\text{mol}/$ ($\text{m}^2 \cdot \text{s}$)	A_n $\mu\text{mol}/$ ($\text{m}^2 \cdot \text{s}$)	C_a (ppmv)
2	HanxiaK195-2-10	50.3	49	20.5	0.5	3.18×10^{-10}	0.314	0.063	0.150	2	-24.22	-5.00	0.596	10	11.5	665
4	HanxiaK195-4-1	58.7	24	16.0	0.5	4.34×10^{-10}	0.222	0.044	0.156	2	-25.10	-5.80	0.600	10	12.0	887
	HanxiaK195-4-29	54.1	40	17.5	0.5	3.72×10^{-10}	0.312	0.062	0.150	2	-25.10	-5.80	0.600	10	11.6	679
Average		56.5	32	16.7	0.5	4.05×10^{-10}	0.265	0.053	0.154	2	-25.10	-5.80	0.600	10	11.8	788
5	HanxiaK195-5-8	35.5	79	11.1	0.5	1.59×10^{-10}	0.410	0.082	0.144	2	-24.94	-5.7	0.599	10	11.1	550
6	HanxiaK195-6-1	35.2	41	7.5	0.5	1.56×10^{-10}	0.252	0.050	0.154	2	-25.60	-6.3	0.602	10	11.9	808

by the recent standardization (531–641 ppmv). Moreover, it is lower than the $p\text{CO}_2$ reconstructed by the Carboniferous standardization (882–1060 ppmv). Overall, the $p\text{CO}_2$ is 665 ppmv for the deposition period of the second member, 788 ppmv for the deposition period of the fourth member, 550 ppmv for the deposition period of the fifth member, and 808 ppmv for the deposition time of the sixth member (Fig. 2 and Table 1). Moreover, the reconstructed $p\text{CO}_2$ showed a significant fluctuation during the four corresponding deposition periods. The $p\text{CO}_2$ first increased during the deposition period of members 2–4, during that time the $p\text{CO}_2$ varied from 665 to 788 ppmv; then, the $p\text{CO}_2$ decreased significantly from 788 to 550 ppmv during the deposition period of members 4–5. Finally, the $p\text{CO}_2$ increased to the peak from 550 to 808 ppmv during the deposition period of members 5–6 (Fig. 3).

5 Discussions

5.1 Comparison and analysis of the previous $p\text{CO}_2$ during the Mid-Cretaceous

At present, the results from reconstruction of the paleo-atmospheric CO_2 concentration in the mid-Cretaceous mainly include the use of plant fossil stomatal parameters (Haworth et al., 2005; Aucour et al., 2008; Ren Wenxiu et al., 2008; Passalia, 2009; Du et al., 2016; Sun Y.W et al., 2016; Dai and Sun, 2017), carbon isotopes of paleosols and fossil liverworts (Ekar et al., 1999; Fletcher et al., 2007; Heimhofer et al., 2004; Wallmann, 2001), biogeochemical models (Bergman et al., 2004; Berner 1994; Berner and Kothavala, 2001; Hansen, 2003; Rothman, 2002; Tajika, 1999), and the newly established mechanical model of plant photosynthetic gas exchange (Franks et al., 2014). The results from this reconstruction are summarized in Table 2 and Fig. 3.

The $p\text{CO}_2$ of the mid-Cretaceous had been

reconstructed frequently based on the fossil Cheirolepidiaceae, especially *Pseudofrenelopsis*, *Brachyphyllum* and *Frenelopsis* by using the SR method (Haworth et al., 2005; Aucour et al., 2008; Ren wenxiu et al., 2008; Passalia, 2009; Du et al., 2016; Dai and Sun, 2017). Haworth et al. (2005) reconstructed the $p\text{CO}_2$ of the early Cretaceous based on the SR of fossil *Pseudofrenelopsis* (Fig. 3). In this reconstruction, the $p\text{CO}_2$ data showed a slightly increasing trend during the early Cretaceous as a whole; the $p\text{CO}_2$ is 696.5–1160.9 ppmv for the middle–late Aptian, 723.7–1206.1 ppmv for the early–middle Albian, indicating a slight rising trend during the late Aptian–early Albian which is similar to the current variation. The $p\text{CO}_2$ values based on the SR method ranged from 531 to 1060 ppmv in Yumen, Gansu Province during the late early Cretaceous, and the $p\text{CO}_2$ showed an overall declining trend within the deposition time of the 2–6 members, which is different from the current result. In detail, the $p\text{CO}_2$ from the third to fifth member is 959–930 ppmv based on the *Pseudofrenelopsis* specimens according to the Carboniferous standardization and 575–558 ppmv according to the recent standardization, respectively. These values indicate that the $p\text{CO}_2$ was relatively stable with no significant variation during the early mid-Cretaceous in the Yumen, Gansu Province. However, the $p\text{CO}_2$ reconstructed based on the *Brachyphyllum* specimens showed a significant decrease (1060–882 ppmv, the Carboniferous standardization; 641–531 ppmv, the recent standardization).

In addition, the stomatal parameters of *Frenelopsis* were measured from the Lower cretaceous collected from eastern and southwestern Spain. The reconstructed $p\text{CO}_2$ was 759–1265 ppmv during the late Barrenmian, 441–736 ppmv during the early Albian, and 505–842 ppmv during the late Albian. The $p\text{CO}_2$ during the latter part of the Early Cretaceous indicated a declining trend and an

Table 2 Summarized $p\text{CO}_2$ results based on the previous and present studies

Age	Species	methods	$p\text{CO}_2$ (ppmv)	References
Hauterivian–Albian	<i>Pseudofrenelopsis</i>	Stomatal ratio	567.5–1206.1	Haworth et al, 2005
Aptian–Albian	<i>Pseudofrenelopsis/Brachyphyllum</i>	Stomatal ratio	531–1060	Du et al, 2015
Middle Aptian	<i>Brachyphyllum</i>	Stomatal ratio	693–1156	Passalia, 2009
Late Albian	<i>Brachyphyllum</i>	Stomatal ratio	740–1232	Passalia, 2009
Late Barrenmian	<i>Frenelopsis</i>	Stomatal ratio	759–1265	Aucour et al, 2008
Early Albian	<i>Frenelopsis</i>	Stomatal ratio	441–736	Aucour et al, 2008
Late Albian	<i>Frenelopsis</i>	Stomatal ratio	505–842	Aucour et al, 2008
Aptian–Santonian	<i>Pseudofrenelopsis</i>	Stomatal ratio	861–1047	Ren et al., 2008
early Middle Aptian–Early Albian	<i>Ginkgo. coriacea</i>	Stomatal ratio	659–1119	Sun et al, 2016
early Middle Aptian– Early Albian	<i>Ginkgo. paradiantoides</i>	Stomatal ratio	677–1142	Sun et al, 2016
Late Hauterivian	<i>Pseudofrenelopsis</i>	Stomatal ratio	595–957	Dai and Sun, 2017
Late Aptian	<i>Pseudofrenelopsis</i>	Stomatal ratio	753–1210	Dai and Sun, 2017
Late Albian	<i>Pseudofrenelopsis</i>	Stomatal ratio	805–1292	Dai and Sun, 2017
Middle Albian (105 Ma)	<i>Araucaria</i>	Gas exchange mechanical model	683	Franks et al, 2014
Late Albian (100 Ma)	<i>Araucaria/Watsoniocladus/Pseudofrenelopsis</i>	Gas exchange mechanical model	1151	Franks et al, 2014
Cenomanian (95 Ma)	<i>Eromanga/Eutactoides/Araucaria/Frenelopsis/Brachyphyllum</i>	Gas exchange mechanical model	878	Franks et al, 2014
Aptian–Albian	<i>Brachyphyllum</i>	Gas exchange mechanical model	550–808	This study

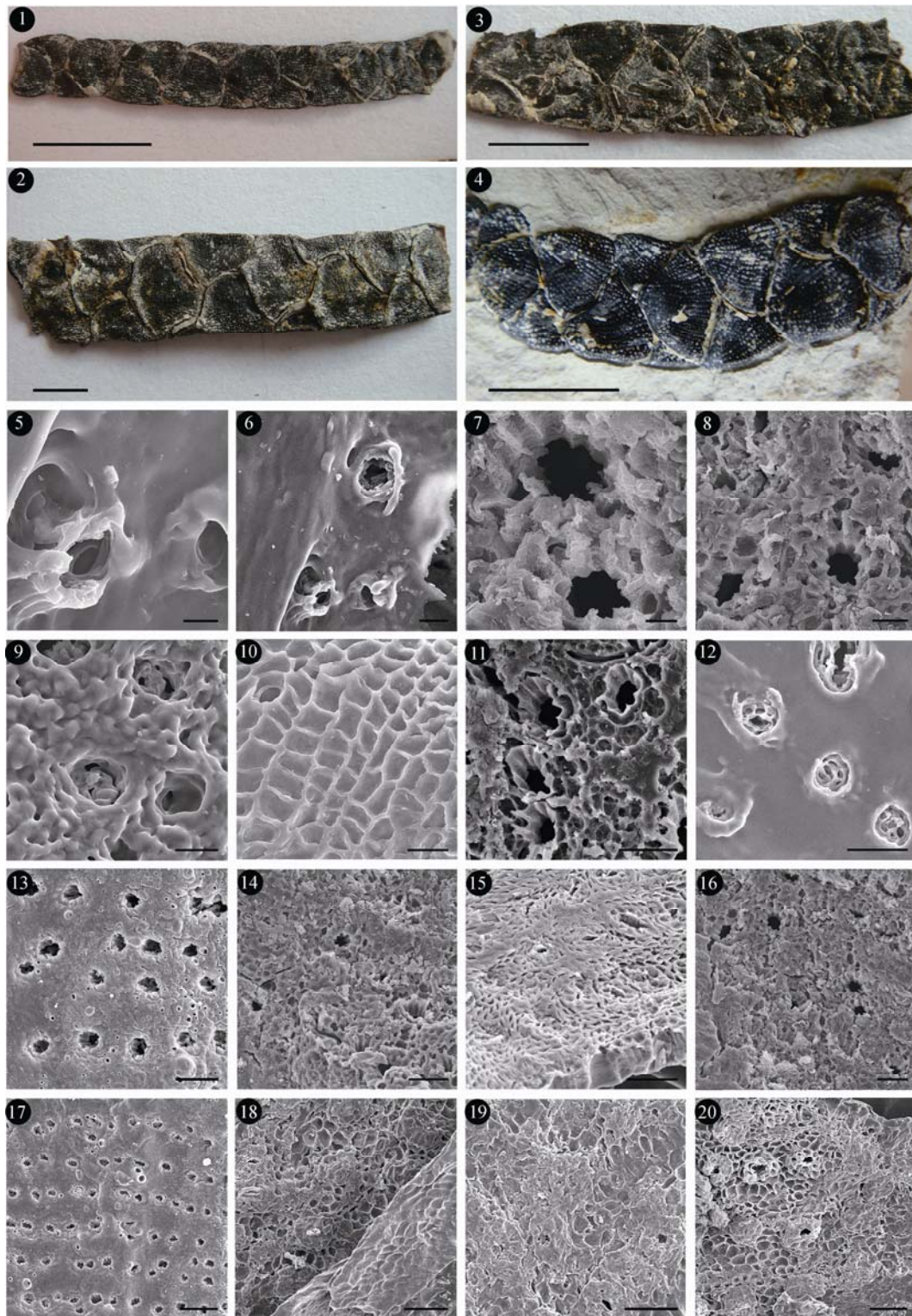


Fig. 2. Fossil specimens and cuticular structures of *Brachyphyllum* from the middle Cretaceous of Yumen, Gansu Province.

Specimen number: 1, HanxiaK195-6-1; 2, HanxiaK195-4-1; 3, HanxiaK195-6-1; 4, HanxiaK195-4-21; 5, 6, 9, HanxiaK195-4-29; 7, 8, 11, 14, 16, HanxiaK195-4-1; 10, 12, 13, 17, HanxiaK195-2-10; 15, HanxiaK195-5-8; 18, 19, 20 HanxiaK195-6-1. Scale bars: 1-4 = 5 mm; 5, 7=20 μ m; 6, 8, 9, 10 = 50 μ m; 11-20 = 100 μ m.

increase in the early part of the middle Cretaceous.

The $p\text{CO}_2$ reconstructed by Passalia (2009) was 693–1156 ppmv based on the *Brachyphyllum* from the Lower

cretaceous of southern Argentina during the middle Aptian, and was 740–1232 ppmv during the late Albian. The reconstruction results also indicate a rising trend

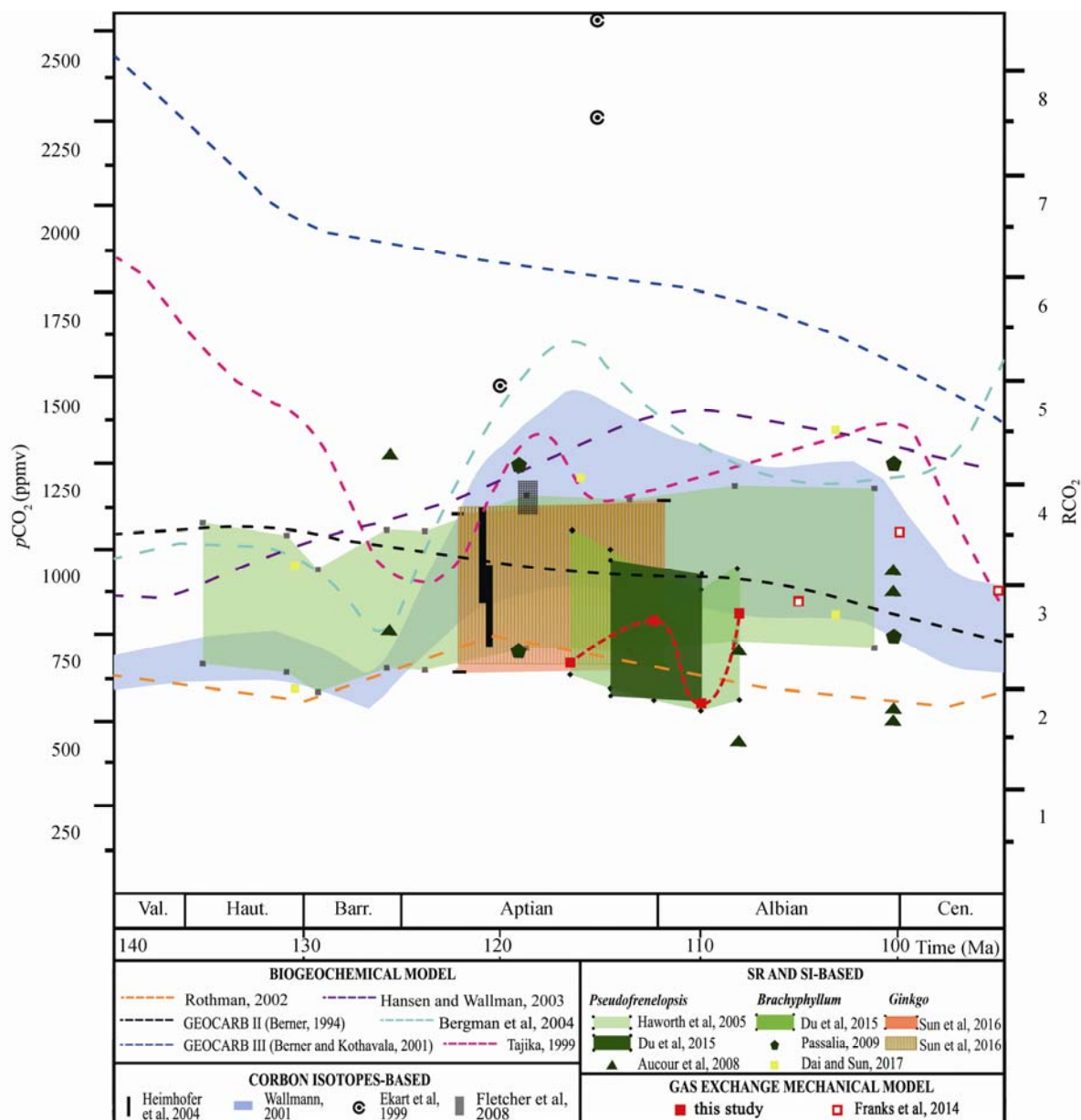


Fig. 3. Middle Cretaceous $p\text{CO}_2$ variation of this study, and previous data based on stomatal parameters, mechanistic model, biogeochemical models and carbon isotopes.

during the middle Cretaceous (the middle Aptian–the late Albian), similar to this study. However, the $p\text{CO}_2$ estimated by Ren et al. (2008) for the middle Cretaceous (the Aptian–the Santonian) was 861–1047 ppmv, which was significantly higher than the reconstruction results in this paper. The $p\text{CO}_2$ from the Fujian and Jiangxi Provinces in southeast China based on the *Pseudofrenelopsis* leaves was 563–701 ppmv based on the recent standardization and was 1022–1314 ppmv based on the Carboniferous standardization during the late Hauterivian–late Aptian, the $p\text{CO}_2$ was 763–1415 ppmv during the late Albian (Dai and Sun, 2017). These results indicated that the atmospheric CO_2 concentration was significantly increasing during the early–middle

Cretaceous, which is also similar to the $p\text{CO}_2$ variation found in this study.

The $p\text{CO}_2$ concentrations can be inferred from either proxies or by the modeling of long-term carbon cycle (Wang et al., 2014). Based on the global carbon cycle models GEOCARB II and GEOCARB III (Berner 1994; Berner and Kothavala, 2001), it was estimated that the $p\text{CO}_2$ showed a relatively steady decline during the late Aptian–early Albian. Our newly acquired data were lower than the $p\text{CO}_2$ obtained using GEOCARB II and GEOCARB III, while all the estimated values were within the scope error of the GEOCARB II and GEOCARB III. In addition, the trend of the paleo-atmospheric CO_2 concentration from late Aptian to early Albian

reconstructed in this paper is similar to the data of the reconstruction in mid-Cretaceous based on the biochemical model put forward by Tajika (1999).

Based on the plant photosynthetic gas exchange mechanical model, the values of paleo-atmospheric CO₂ concentrations was recovered in the middle Cretaceous (105, 100, and 95 Ma) by Franks et al. (2014). When these values are combined with those of the current results, we found that the global CO₂ concentration show a significant increasing during the late Aptian to latest Albian, and the *p*CO₂ reached its peak during the early Cenomanian, and then decreased significantly after. The *p*CO₂ in the Aptian–Cenomanian indicated that a trend of first rising and then decreasing as a whole, which corresponded to a significant increase of greenhouse warming in the middle Cretaceous; the increasing variation of *p*CO₂ during the early middle Cretaceous can also be supported by the results of Haworth et al. (2005), Aucour et al. (2008), Passalia (2009) and Dai and Sun (2017).

5.2 Relation between *p*CO₂ and OAE1b during the Mid-Cretaceous

The oceanic anoxic events of the Cretaceous are characterized by many instances of oxygen-deficient ocean bottom water, thereby resulting in deposits of organic-rich black shales in various ocean basins worldwide (Schlanger and Jenkyns, 1976; Jenkyns, 2003; Huang Yongjian and Wang Chengshan, 2008). The black shales formed in the Cretaceous oceanic anoxic environments also constitute the source rock of many large oil fields, such as the Middle East, North Sea, and Siberia (Hu Xiumian, 2004). Therefore, the oceanic anoxic event in the Cretaceous is of great significance in the studies of geosciences. It changed the lithological, biological, and geochemical characteristics of oceanic and terrestrial environments (Wan Xiaoqiao, 1992; Wan Xiaoqiao et al., 2005; Dai Shuang et al., 2012).

The relation between the *p*CO₂ changes and oceanic anoxic events has been discussed previously, and the burial of large amounts of organic carbon caused by successive oceanic anoxic events has had a profound impact on the atmosphere-ocean system (Huang Yongjian and Wang Chengshan, 2008). The oceanic anoxic events are also closely related to the major perturbations of the global carbon cycle (Wang et al., 2014). The results of Arthur et al. (1988) indicate that the oceanic anoxic events are often associated with the excursions of the δ¹³C values of the ocean sediments.

The mid-Cretaceous period was the most frequent period of oceanic anoxic events (Aptian–Albian), and four oceanic anoxic events occurred successively, including OA1a (Selli layer, 120 Ma), OAE1b (ca. 109–113 Ma),

OAE1c (ca. 102 Ma), and OAE1d (ca. 99 Ma) (Follmi, 2012). In detail, OAE1a occurred in the early Aptian, and is considered to be a period of accumulation of organic carbon-rich marine sediments on a global scale (Mehay et al., 2009); this is a paleoceanic productivity event and marks the beginning of the Cretaceous greenhouse climate (Huang Yongjian and Wang Chengshan, 2008). OAE1b occurred from the late Aptian to the early Albian and represents a significant shift of the tectonic setting, sea level, climate, lithofacies, and marine plankton communities in the mid-Cretaceous (Leckie et al., 2002). In addition, the period was accompanied by a rapid decline of sea level (Weissert and Lini, 1991; Weissert et al., 1998; Leckie et al., 2002).

Weissert and Lini (1991) argue that the global cooling, glacier developments and sea level drop led to the negative values of δ¹³C during the middle–late Aptian. The δ¹³C values of the *Brachyphyllum* specimens represent a negative shift during the transition period between the Aptian and Albian (Du et al., 2016), and the variation is quite similar to the change of the isotopic values of marine carbonate rocks measured by Weissert et al. (1998) during the OAE1b period, which may provide an evidence that terrestrial plants can also respond to the oceanic anoxic events. In addition, the δ¹³C values of charcoal from the early Toarcian (Lower Jurassic) also demonstrated a negative excursion and are considered a response to the oceanic anoxic event (Deng Shenghui et al., 2012a). Therefore, the terrestrial ecosystems, especially plants, can impart or respond to the oceanic climate events.

The relation between the *p*CO₂ and ocean anoxic events is still in the exploration and assessment stages. Most of the *p*CO₂ reconstructed by fossil plants are low in temporal resolution, which limits the accurate identification of changes in the short term. So, it is difficult to determine the causality between OAEs and CO₂ concentration based on plant fossils (Sun Y.W et al., 2016). Sun Y.W et al., (2016) attempted to clarify the relation between the variation of *p*CO₂ and OAEs using the fossil *Ginkgo* from the Lower Cretaceous of northeast China based on both SR and SI methods. The SR method offered a result of 659–671 ppmv according to the recent standardization or 1098–1119 ppmv according to the Carboniferous standardization of the Changcai Formation (125.1–116.8 Ma), and 677–685 ppmv according to the recent standardization or 1128–1142 ppmv according to the Carboniferous standardization of the Yingcheng Formation (115–110 Ma). However, the SI method offered a result of 970–1065 ppmv for the Changcai Formation and 1152–1305 ppmv for the Yingcheng Formation; and the small rise of *p*CO₂ might indicate a response of fossil

plants to the OAE 1b. The $p\text{CO}_2$ values of this study also indicate an overall rising trend during the late Aptian–Early Albian, while the $p\text{CO}_2$ fluctuated obviously, which indicates that the terrestrial $p\text{CO}_2$ changed dramatically during the OAEs.

5.3 Relation between the $p\text{CO}_2$ variation and Cold snap event during the mid-Cretaceous

The mid-Cretaceous (Aptian–Turonian, 120–90 Ma) is characterized by greenhouse warming. During this period, the global temperatures are rising to the peak and sea levels are elevated (Haq et al., 1987; Mutterlose et al., 2009; Wilson et al., 2002). While the climate was not stable but fluctuated between hot- and cool-warm (Wang et al., 2014), Bodin et al. (2015) studied the oxygen, carbon, and strontium isotopes in the marine sediments in the southeast part of France, which demonstrated that there are short period coolings in the late Valanginian to the early Hauterivian, the middle Aptian, and the transition period between the Aptian and Albian. The Cold snap event happened during the late Aptian to the early Albian is recorded as a significant global cooling event, influenced by this event, ocean biota restructured, i.e., thermophilic calcareous ultramicrobe declined in the high and low latitudes, while cold water species, such as the ultramicrobe and psychrophilic ones, arose in the high latitudes (Mutterlose et al., 2009). In addition, deposits of psychrophilic glauconite calcite mineral were frequently found from the late Aptian–the early Albian strata in the Sverdrup and Svalbard basins of Canada and south-east of Australia (Frakes et al., 1995; Mutterlose et al., 2009). According to the analysis by Mcanena et al. (2013) and Herrle et al. (2015) of the organic carbon and carbon isotopic composition in the core sediments and TEX86 in the eastern Atlantic and the sediments in the Atlantic, it is found that sea surface temperatures dropped by about 4–5°C across the Aptian and the Albian boundary.

The carbon isotopic data showed that the accumulation of organic carbon in this period increased significantly, which resulted in the decrease of atmospheric CO_2 concentration and cooling of climate (Arthur et al., 1988; Kaiho et al., 1994; Kuypers et al., 1999; Turgeon and Creaser, 2008). Studies based on Antarctic ice core have confirmed the relationship between the global CO_2 concentration change and temperature changes since the late Quaternary (Pedro, 2012). As a typical greenhouse gas, the CO_2 concentration variation is not only related to long-term climate change but also closely related to the short-term global climate events (Hong and Lee, 2012). As during the greenhouse climate period, high temperature accelerated the global hydrologic cycle, causing the increased nutrient supply derived from the mainland

(Jenkyns, 2010) and increasing the productivity of the ocean; this process favors the organic matter sedimentary, absorbing CO_2 from the atmosphere and thereby leading to a reduction in atmospheric CO_2 concentration. This process had a negative effect on the global temperature, causing the down trend of the global temperature.

In this study, the reconstructed $p\text{CO}_2$ are relatively lower in comparison with the other $p\text{CO}_2$ values of similar stages (Fig. 3), and the $p\text{CO}_2$ showed a distinct fluctuation during the late Aptian to the early Albian time. A distinct decreasing trend was recognized within the sedimentary period of members 4–5. So, the present decline in $p\text{CO}_2$ may indicate a short-term cooling, and may be a response to the Cold snap event in transitional period of the Aptian to the Albian. The Cold snap event is not necessarily caused by the reduction in the atmospheric CO_2 concentration, but Cold snap events are often accompanied by a reduction in the atmospheric CO_2 concentration (Bottini et al., 2015).

6 Conclusions

(1) The paleo-atmospheric CO_2 concentrations in Yumen, Gansu Province during the late Aptian–early Albian were reconstructed based on the plant photosynthetic gas exchange mechanistic models using the fossil specimens of *Brachyphyllum*. The estimated $p\text{CO}_2$ was 550–808 ppmv, which is between the results obtained using the SR method. The $p\text{CO}_2$ values are also within the error range of the GEOCARB II and GEOCARB III.

(2) The $p\text{CO}_2$ showed an overall increasing trend during the late Aptian–early Albian in the Yumen Gansu province, and the $p\text{CO}_2$ fluctuated with a first increasing, then decreasing, and finally an increasing trend during the sedimentary period of the member 2–6.

(3) The present $p\text{CO}_2$ variation can be related to some climatic events during the middle Cretaceous (Aptian–Cenomanian), an overall increasing trend of $p\text{CO}_2$ may indicate greenhouse warming during the middle Cretaceous, and the fluctuation of $p\text{CO}_2$ may be connected with the OAE 1b. In addition, the decreasing trend during the sedimentary period of the member 4–5 may be connected with the Cold snap event during the transition of the Aptian and Albian.

Acknowledgements

This work was conducted under the National Natural Science Foundation of China (No. 41402007; 41602023; 40972025), and the State Key Laboratory of Palaeobiology and Stratigraphy, Nanjing Institute of Geology and Palaeontology, CAS (No.153102).

Manuscript received Feb. 15, 2018

accepted Mar. 10, 2018

edited by Liu Lian

References

- Arens, N.C., Jahren, A.H., and Amundson, R., 2000. Can C₃ plants faithfully record the carbon isotopic composition of atmospheric carbon dioxide? *Paleobiology*, 26(1): 137–164.
- Arthur, M.A., Dean, W.E., and Pratt, L.M., 1988. Geochemical and climatic effects of increased marine organic carbon burial at the Cenomanian/Turonian boundary. *Nature*, 335(6192): 714–717.
- Aucour, A.M., Gomez, B., Sheppard, S.M.F., and Thévenard, F., 2008. $\delta^{13}\text{C}$ and stomatal number variability in the Cretaceous conifer *Frenelopsis*. *Palaeogeography, Palaeoclimatology, Palaeoecology*, 257(4): 462–473.
- Beerling, D.J., Fox, A., and Anderson, C.W., 2009. Quantitative uncertainty analyses of ancient atmospheric CO₂ estimates for fossil leaves. *Polskie Archiwum Medycyny Wewnatrznej*, 309(9): 349–354.
- Beerling, D.J., Lomax, B.H., Royer, D.L., Jr, U.G., and Kump, L.R., 2002. An atmospheric pCO₂ reconstruction across the Cretaceous-Tertiary boundary from leaf megafossils. *Proceedings of the National Academy of Sciences of the United States of America*, 99(12): 7836–7840.
- Bergman, N.M., Lenton, T.M., and Watson, A.J., 2004. COPSE: A new model of biogeochemical cycling over Phanerozoic time. *American Journal of Science*, 304(5): 397–437.
- Berner, R.A., 1994. Geocarb II: A revised model of atmospheric CO₂ over Phanerozoic time. *American Journal of Science*, 294: 56–91.
- Berner, R.A., and Kothavala, Z., 2001. Geocarb III: A revised model of atmospheric CO₂ over Phanerozoic time. *American Journal of Science*, 301(2): 182–204.
- Bodin, S., Meissner, P., Janssen, N.M.M., Steuber, T., and Mutterlose, J., 2015. Large igneous provinces and organic carbon burial: Controls on global temperature and continental weathering during the Early Cretaceous. *Global and Planetary Change*, 133: 238–253.
- Bonis, N.R., and Kürschner, W.M., 2010. Changing CO₂ conditions during the end-Triassic inferred from stomatal frequency analysis on *Lepidopteris ottonis* (Goepfert) Schimper and *Ginkgoites taeniatus* (Braun) Harris. *Palaeogeography, Palaeoclimatology, Palaeoecology*, 295(1): 146–161.
- Bottini, C., Erba, E., Tiraboschi, D., Jenkyns, H.C., Schouten, S., and Sinninghe Damsté, J.S., 2015. Climate variability and ocean fertility during the Aptian Stage. *Climate of the Past*, 11(3): 383–402.
- Came, R.E., Eiler, J.M., Veizer, J., Azmy, K., Brand, U., and Weidman, C.R., 2007. Coupling of surface temperatures and atmospheric CO₂ concentrations during the Palaeozoic era. *Nature*, 449(7159): 198–201.
- Cronin, M., Tauxe, L., Constable, C., Selkin, P., and Pick, T., 2001. Noise in the quiet zone. *Earth and Planetary Science Letters*, 190(1–2): 13–30.
- Dai, J., and Sun, B.N., 2017. Early Cretaceous atmospheric CO₂ estimates based on stomatal index of *Pseudofrenelopsis papillosa* (Cheirolepidiaceae) from southeast China. *Cretaceous Research*, 85: 232–242.
- Dai Shuang, Liu Xue, Zhao Jie, Zhang Mingzhen, Liu Junwei, Kong Li, Zhu Qiang and Huang Yongbo, 2012. The OAEs record in the terrestrial sediments: The geochemistry of blackshales in the Liupanshan Group and its paleoclimatic implications. *Earth Science Frontiers*, 19(4): 255–259 (in Chinese with English abstract).
- Deng, S.H., Yang, X.J., and Lu, Y.Z., 2005. *Pseudofrenelopsis* (Cheirolepidiaceae) from the Lower Cretaceous of Jiuquan, Gansu, northwestern China. *Acta Palaeontologica Sinica* (English Edition), 44(4): 505–516.
- Deng Shenghui and Lu Yuanzheng, 2008. Fossil plants from lower Cretaceous of the Jiuquan Basin, Gansu, Northwest China and their palaeoclimatic implications. *Acta Geologica Sinica*, 82: 104–114 (in Chinese with English abstract).
- Deng Shenghui, Lu Yuanzheng, Fan Ru, Fang Linhao, Li Xin and Liu Lu, 2012a. Toarcian (Early Jurassic) Oceanic Anoxic Event and the responses in terrestrial ecological system. *Earth Science*, 37(s2): 23–38 (in Chinese with English abstract).
- Deng Shenghui, Lu Yuanzheng, Fan Ru, Li Xin, Fang Linhao and Liu Lu, 2012b. Cretaceous floras and biostratigraphy of China. *Journal of Stratigraphy*, 36(2): 241–265 (in Chinese with English abstract).
- Du, B.X., Sun, B.N., Zhang, M.Z., Yang, G.L., Xing, L.T., Tang, F.J., and Bai, Y.X., 2016. Atmospheric palaeo-CO₂ estimates based on the carbon isotope and stomatal data of Cheirolepidiaceae from the Lower Cretaceous of the Jiuquan Basin, Gansu Province. *Cretaceous Research*, 62: 142–153.
- Du, B.X., Zhang, M.Z., Dai, S., and Sun, B.N., 2014. Discovery of *Pseudofrenelopsis* from the Lower Cretaceous of Liupanshan Basin and its paleoclimatic significance. *Cretaceous Research*, 48(1): 193–204.
- Ekart, D.D., Cerling, T.E., Montañez, I.P., and Tabor, N.J., 1999. A 400 million year carbon isotope record of pedogenic carbonate: Implications for paleoatmospheric carbon dioxide. *American Journal of Science*, 299(10): 805–827.
- Epron, D., Godard, D., Cornic, G., and Genty, B., 1995. Limitation of net CO₂ assimilation rate by internal resistances to CO₂ transfer in the leaves of two tree species (*Fagus sylvatica* L. and *Castanea sativa* Mill.). *Plant Cell & Environment*, 18(1): 43–51.
- Evans, J.R., and Caemmerer, S.V., 1996. Carbon dioxide diffusion inside leaves. *Plant Physiology*, 110(2): 339.
- Farquhar, G.D., and Sharkey, T.D., 1982. Stomatal conductance and photosynthesis. *Annual Reviews of Plant Physiology*, 33(33): 317–345.
- Fletcher, B.J., Brentnall, S.J., Anderson, C.W., Berner, R.A., and Beerling, D.J., 2007. Atmospheric carbon dioxide linked with Mesozoic and early Cenozoic climate change. *Nature Geoscience*, 1(1): 43–48.
- Follmi, K.B., 2012. Early Cretaceous life, climate and anoxia. *Cretaceous Research*, 35(35): 230–257.
- Frakes, L.A., Alley, N.F., and Deynoux, M., 1995. Early Cretaceous ice rafting and climate zonation in Australia. *International Geology Review*, 37(7): 567–583.
- Franks, P.J., and Beerling, D., 2009. Maximum leaf conductance driven by CO₂ effects on stomatal size and density over geologic time. *Proceedings of the National Academy of Sciences of the United States of America*, 106(25): 10343–10347.
- Franks, P.J., Drake, P.L., and Beerling, D., 2009. Plasticity in maximum stomatal conductance constrained by negative

- correlation between stomatal size and density: an analysis using *Eucalyptus globulus*. *Plant Cell & Environment*, 32(12): 1737–1748.
- Franks, P.J., Leitch, I.J., Ruzsala, E.M., Hetherington, A.M., and Beerling, D.J., 2012. Physiological framework for adaptation of stomata to CO₂ from glacial to future concentrations. *Philosophical Transactions of the Royal Society of London*, 367(1588): 537–546.
- Franks, P.J., Adams, M.A., Amthor, J.S., Barbour, M.M., Berry, J.A., Ellsworth, D.S., Farquhar, G.D., Ghannoum, O., Lloyd, J., and McDowell, N., 2013. Sensitivity of plants to changing atmospheric CO₂ concentration: from the geological past to the next century. *New Phytologist*, 197(4): 1077–1094.
- Franks, P.J., Royer, D.L., Beerling, D.J., Water, P.K.V.D., Cantrill, D.J., Barbour, M.M., and Berry, J.A., 2014. New constraints on atmospheric CO₂ concentration for the Phanerozoic. *Geophysical Research Letters*, 41(13): 4685–4694.
- Grein, M., Konrad, W., Wilde, V., Utescher, T., and Roth-Nebelsick, A., 2011. Reconstruction of atmospheric CO₂ during the early middle Eocene by application of a gas exchange model to fossil plants from the Messel Formation, Germany. *Palaeogeography, Palaeoclimatology, Palaeoecology*, 309(3–4): 383–391.
- Grein, M., Oehm, C., Konrad, W., Utescher, T., Kunzmann, L., and Roth-Nebelsick, A., 2013. Atmospheric CO₂ from the late Oligocene to early Miocene based on photosynthesis data and fossil leaf characteristics. *Palaeogeography, Palaeoclimatology, Palaeoecology*, 374: 41–51.
- Hansen, K.W., 2003. Cretaceous and Cenozoic evolution of seawater composition, atmospheric O₂ and CO₂: A model perspective. *American Journal of Science*, 303(2): 94–148.
- Haq, B.U., Hardenbol, J., and Vail, P.R., 1987. Chronology of Fluctuating Sea Levels Since the Triassic. *Science*, 235(4793): 1156.
- Haworth, M., Hesselbo, S.P., McElwain, J.C., Robinson, S.A., and Brunt, J.W., 2005. Mid-Cretaceous pCO₂ based on stomata of the extinct conifer *Pseudofrenelopsis* (Cheirolepidiaceae). *Geology*, 33(9): 749.
- Heimhofer, U., Hochuli, P.A., Herrle, J.O., Andersen, N., and Weissert, H., 2004. Absence of major vegetation and palaeoatmospheric pCO₂ changes associated with oceanic anoxic event 1a (Early Aptian, SE France). *Earth and Planetary Science Letters*, 223(3–4): 303–318.
- Helsley, C.E.S., and Maureen, B., 1968. Evidence for long intervals of normal polarity during the cretaceous period. *Earth and Planetary Science Letters*, 5: 325–332.
- Herrle, J.O., Schröder-Adams, C.J., Davis, W., Pugh, A.T., Galloway, J.M., and Fath, J., 2015. Mid-Cretaceous High Arctic stratigraphy, climate, and Oceanic Anoxic Events. *Geology*, 43(5): 403–406.
- Hong, S.K., and Lee, Y.I., and Yi, S., 2012. Carbon isotopic composition of terrestrial plant matter in the Upper Cretaceous Geoncheonri Formation, Gyeongsang Basin, Korea: Implications for Late Cretaceous palaeoclimate on the East Asian continental margin. *Cretaceous Research*, 35: 169–177.
- Hu Xiumian, 2004. Greenhouse climate and ocean during the Cretaceous. *Geology in China*, 31(4): 442–448 (in Chinese with English abstract).
- Huang Yongjian and Wang Chengshan, 2008. Cretaceous Oceanic Anoxic Event: Research Progress and forthcoming prospects. *Acta Geologica Sinica*, 82(1): 21–30 (in Chinese with English abstract).
- Huang, C.M., Retallack, G.J., and Wang, C.S., 2012. Early Cretaceous atmospheric pCO₂ levels recorded from pedogenic carbonates in China. *Cretaceous Research*, 33(1): 42–49.
- Jenkyns, H.C., 1980. Cretaceous anoxic events: from continents to oceans. *Journal of the Geological Society*, 137(2): 171–188.
- Jenkyns, H.C., 2003. Evidence for rapid climate change in the Mesozoic-Palaeogene greenhouse world. *Philosophical Transactions: Mathematical, Physical and Engineering Sciences*, 361(1810): 1885–1916.
- Jenkyns, H.C., 2010. Geochemistry of oceanic anoxic events. *Geochemistry Geophysics Geosystems*, 11(3): 10.1029/2009GC002788.
- Jin, P.H., Mao, T., Dong, J.L., Wang, Z.X., Sun, M.X., Xu, X.H., Du B.X., and Sun, B.N., 2017. A new species of *Cupressinocladus* from the Lower Cretaceous of Guyang Basin, Inner Mongolia, China and cluster analysis. *Acta Geologica Sinica* (English Edition), 91(4): 1215–1230.
- Jones, C.E., 2001. Seawater strontium isotopes, oceanic anoxic events, and seafloor hydrothermal activity in the Jurassic and Cretaceous. *American Journal of Science*, 301(2): 112–149.
- Jordan, G.J., 2011. A critical framework for the assessment of biological palaeoproxies: predicting past climate and levels of atmospheric CO₂ from fossil leaves. *New Phytologist*, 192(1): 29–44.
- Kürschner, W.M., Kvaček, Z., and Dilcher, D.L., 2008. The impact of Miocene atmospheric carbon dioxide fluctuations on climate and the evolution of terrestrial ecosystems. *Proceedings of the National Academy of Sciences of the United States of America*, 105(2): 449–453.
- Kürschner, W.M., Stulen, I., Wagner, F., and Kuiper, P.J.C., 1998. Comparison of palaeobotanical observations with experimental data on the leaf anatomy of Durmast Oak [*Quercus petraea* (Fagaceae)] in response to environmental change. *Annals of Botany*, 81(5): 657–664.
- Kaiho, K., and Hasegawa, T., 1994. End-Cenomanian benthic foraminiferal extinctions and oceanic dysoxic events in the northwestern Pacific Ocean. *Palaeogeography, Palaeoclimatology, Palaeoecology*, 111(1–2): 29–43.
- Katz, M., Cramer, B., Franzese, A., Honisch, B., Miller, K., Rosenthal, Y., and Wright, J., 2010. Traditional and emerging geochemical proxies in foraminifera. *Journal of Foraminiferal Research*, 40(2): 165–192.
- Konrad, W., Roth-Nebelsick, A., and Grein, M., 2008. Modelling of stomatal density response to atmospheric CO₂. *Journal of Theoretical Biology*, 253(4): 638–658.
- Kuypers, M.M.M., Pancost, R.D., and Damsté, J.S.S., 1999. A large and abrupt fall in atmospheric CO₂ concentration during Cretaceous times. *Nature*, 399(6734): 342–345.
- Larson, R.L., 1991. Latest pulse of Earth: Evidence for a mid-Cretaceous superplume. *Geology*, 19(6): 547–550.
- Leckie, R.M., Bralower, T.J., and Cashman, R., 2002. Oceanic anoxic events and plankton evolution: Biotic response to tectonic forcing during the mid-Cretaceous. *Paleoceanography*, 17(3): 1–29.
- Li, X.H., Jenkyns, H.C., Zhang, C.K., Wang, Y., Liu, L., and Cao, K., 2013. Carbon isotope signatures of pedogenic carbonates from SE China: rapid atmospheric pCO₂ changes during middle-late Early Cretaceous time. *Geological*

- Magazine*, 151(5): 830–849.
- Li, R.Y., Wang, X.L., Jin, P.H., Ma, F.J., Yan, D.F., Lin, Z.C., and Sun, B.N., 2016. Fossil liverworts from the Lower Cretaceous Huolinhe Formation in Inner Mongolia, China. *Acta Geologica Sinica* (English Edition), 90(3): 838–846.
- Mann, M.E., Bradley, R.S., and Hughes, M.K., 1999. Northern hemisphere temperatures during the past millennium: Inferences, uncertainties, and limitations. *Geophysical Research Letters*, 26(6): 759–762.
- Mann, M., Amman, C., Bradley, R., Briffa, K., Jones, P., Osborn, T., Crowley, T., Hughes, M., Oppenheimer, M., and Overpeck, J., 2013. On past temperatures and anomalous late-20th-century warmth. *Eos Transactions American Geophysical Union*, 84(27): 256–256.
- Mcanena, A., Flögel, S., Hofmann, P., Herrle, J.O., Griesand, A., Pross, J., Talbot, H.M., Rethemeyer, J., Wallmann, K., and Wagner, T., 2013. Atlantic cooling associated with a marine biotic crisis during the mid-Cretaceous period. *Nature Geoscience*, 6(7): 558–561.
- Mcelwain, J.C., and Chaloner, W.G., 1995. Stomatal density and index of fossil plants track atmospheric carbon dioxide in the Palaeozoic. *Annals of Botany*, 76(4): 389–395.
- Mehay, S., Keller, C.E., Bernasconi, S.M., Weissert, H., Erba, E., Bottini, C., and Hochuli, P.A., 2009. A volcanic CO₂ pulse triggered the Cretaceous Oceanic Anoxic Event 1a and a biocalcification crisis. *Geology*, 37(9): 819–822.
- Mehrotra, R.C., Tewari, R., and Joshi, A., 2003. Application of fossil cuticles in determining palaeoatmospheric CO₂ concentration. *Current Science*, 84(1): 93–94.
- Mutterlose, J., Bornemann, A., and Herrle, J., 2009. The Aptian–Albian cold snap: Evidence for "mid" Cretaceous icehouse interludes. *Neues Jahrbuch für Geologie und Paläontologie-Abhandlungen*, 252(2): 217–225.
- Pagani, M., 2002. The alkenone-CO₂ proxy and ancient atmospheric carbon dioxide. *Philosophical Transactions: Mathematical, Physical and Engineering Sciences*, 360(1793): 609–632.
- Passalia, M.G., 2009. Cretaceous pCO₂ estimation from stomatal frequency analysis of gymnosperm leaves of Patagonia, Argentina. *Palaeogeography, Palaeoclimatology, Palaeoecology*, 273(1–2): 17–24.
- Pedro, J.B., 2012. Tighter constraints on the relative timing of the temperature and atmospheric CO₂ increase during the last deglaciation. *Quaternary International*, 279–280(34): 372–372.
- Ren Wenxiu, Sun Bainian, Wu Jingyu, Xiao Liang and Wang Yongdong, 2008. Microstructures of two species of Cheirolepidiaceae from cretaceous in Zhejiang China and its paleoenvironmental significance. *Acta Geologica Sinica*, 82(5): 577–583 (in Chinese with English abstract).
- Retallack, G.J., 2001. A 300-million-year record of atmospheric carbon dioxide from fossil plant cuticles. *Nature*, 411(6835): 287–290.
- Roeske, C.A., and O'Leary, M.H., 1984. Carbon isotope effects on enzyme-catalyzed carboxylation of ribulose biphosphate. *Biochemistry*, 23(25): 6275–6284.
- Roth-Nebelsick, A., Grein, M., Utescher, T., and Konrad, W., 2012. Stomatal pore length change in leaves of *Eotrigonobalanus furcinervis* (Fagaceae) from the Late Eocene to the Latest Oligocene and its impact on gas exchange and CO₂ reconstruction. *Review of Palaeobotany & Palynology*, 174(6): 106–112.
- Roth-Nebelsick, A., Oehm, C., Grein, M., Utescher, T., Kunzmann, L., Friedrich, J.P., and Konrad, W., 2014. Stomatal density and index data of *Platanus neptuni* leaf fossils and their evaluation as a CO₂ proxy for the Oligocene. *Review of Palaeobotany and Palynology*, 206(4): 1–9.
- Rothman, D.H., 2002. Atmospheric carbon dioxide levels for the last 500 million years. *Proceedings of the National Academy of Sciences of the United States of America*, 99(7): 4167–4171.
- Royer, D.L., Berner, R.A., Montañez, I.P., Tabor, N.J., and Beerling, D.J., 2004. CO₂ as a primary driver of Phanerozoic climate. *GSA Today*, 14(3): 4–10.
- Schlanger, S.O., and Jenkyns, H.C., 1976. Cretaceous Oceanic Anoxic Events: Causes and consequences: Causes and consequences. *Geologie En Mijnbouw*, 55(3–4): 179–184.
- Sun, B.N., Du, B.X., Ferguson, D.K., Chen, J.L., He, Y.L., and Wang, Y.D., 2013. Fossil *Equisetum* from the Lower Cretaceous in Jiuquan Basin, Gansu, Northwest China and its paleoclimatic significance. *Palaeogeography, Palaeoclimatology, Palaeoecology*, 385(1): 202–212.
- Sun, B.N., Wang, Q.J., Konrad, W., Ma, F.J., Dong, J.L., and Wang, Z.X., 2016. Reconstruction of atmospheric CO₂ during the Oligocene based on leaf fossils from the Ningming Formation in Guangxi, China. *Palaeogeography, Palaeoclimatology, Palaeoecology*, 467(1): 5–15.
- Sun, Y.W., Li, X., Zhao, G.W., Liu, H., and Zhang Y.L., 2016. Aptian and Albian atmospheric CO₂ changes during oceanic anoxic events: Evidence from fossil *Ginkgo* cuticles in Jilin Province, Northeast China. *Cretaceous Research*, 62: 130–141.
- Tajika, E., 1999. Carbon cycle and climate change during the Cretaceous inferred from a biogeochemical carbon cycle model. *Island Arc*, 8(2): 293–303.
- Turgeon, S.C., and Creaser, R.A., 2008. Cretaceous oceanic anoxic event 2 triggered by a massive magmatic episode. *Nature*, 454(7202): 323–326.
- Wallmann, K., 2001. Controls on the cretaceous and cenozoic evolution of seawater composition, atmospheric CO₂ and climate. *Geochimica et Cosmochimica Acta*, 65(18): 3005–3025.
- Wan Xiaoqiao, 1992. Introduction to the Cretaceous Oceanic Anoxic Event. *Geological Science and Technology Information*, 11(1): 35–40 (in Chinese with English abstract).
- Wan Xiaoqiao, Li Gang, Chen Peiji, Yu Tao and Ye Dequan, 2005. Isotope stratigraphy of the Cretaceous Qingshankou Formation in Songliao basin and its correlation with Marine Cenomanian stage. *Acta Geologica Sinica*, 79(2): 150–156 (in Chinese with English abstract).
- Wang, Y.D., Huang, C.M., Sun, B.N., Quan, C., Wu, J.Y., and Lin, Z.C., 2014. Paleo-CO₂ variation trends and the Cretaceous greenhouse climate. *Earth-Science Reviews*, 129: 136–147.
- Weislogel, A., Graham, S., and Chamberlain, C.P., 2008. Reconstruction of Late Permian-Mesozoic pCO₂ from δ¹³C composition of pedogenic carbonate, Ordos and Sichuan Basins of Central China. *Geological Society of America Abstracts with Programs*, 40: 259.
- Weissert, H., and Lini, A., 1991. Ice age interludes during the time of Cretaceous greenhouse climate. *Controversies in Modern Geology*, 173–191.

- Weissert, H., Lini, A., Föllmi, K.B., and Kuhn, O., 1998. Correlation of Early Cretaceous carbon isotope stratigraphy and platform drowning events: a possible link? *Palaeogeography, Palaeoclimatology, Palaeoecology*, 137(3–4): 189–203.
- Wilson, P.A., Norris, R.D., and Cooper, M.J., 2002. Testing the Cretaceous greenhouse hypothesis using glassy foraminiferal calcite from the core of the Turonian tropics on Demerara Rise. *Geology*, 30(7): 607–610.
- Xie Shucheng, Yang Huan, Dang Xinyue and Wang Canfa, 2018. Some issues in microbial responses to environmental change and the application of molecular proxies. *Geological Review*, 64(1): 183–189 (in Chinese with English abstract).
- Zhang, M.Z., Ji, L.M., Du, B.X., Dai, S., and Hou, X.W., 2015. Palynology of the Early Cretaceous Hanxia Section in the Jiuquan Basin, Northwest China: The discovery of diverse early angiosperm pollen and paleoclimatic significance. *Palaeogeography, Palaeoclimatology, Palaeoecology*, 440: 297–306.
- Zheng, D.R., Zhang, H.C., Zhang, Q., Li, S., Wang, H., Fang, Y., Liu, Q., Jarzembowski, E.A., Yan, E., and Wang, B., 2015. The discovery of an Early Cretaceous dragonfly *Hemeroscopus baissicus* Pritykina, 1977 (Hemeroscopidae) in Jiuquan, Northwest China, and its stratigraphic implications. *Cretaceous Research*, 52: 316–322.

About the first author

LEI Xiangtong, male; born in 1994 in Dingxi City, Gansu Province; master student; study in Lanzhou university. He is now interesting in the study on the paleobotany and the paleoclimate in the Mesozoic. Email: leixt16@lzu.edu.cn.